Rev. Roum. Sci. Techn.– Électrotechn. et Énerg.
Vol. **71**, *1*, pp. 65–70, Bucarest, 2026

SIMULATION AND EXPERIMENTAL INVESTIGATION OF A COUPLED-INDUCTOR BASED LED DRIVER CIRCUIT

MURALI DURAISAMY

Keywords: DC-DC buck topology; Double pulse width modulation (PWM) technique; Light-emitting diode (LED) driver circuit; Prototype model; PSIM; Zero-voltage switching (ZVS).

A light-emitting diode (LED) or an LED string can receive a regulated power input from highly efficient, low-cost LED driver topologies using a simple control strategy. The presented work elucidates the analysis of a DC-DC buck topology-based single-stage LED driver circuit with dual output voltage levels. The projected driver structure has a reduced semiconductor-based component count and can control the LED light output. The suggested driver circuit employs a magnetically coupled inductor for transformerless energy transfer. The power switches employed in the proposed structure use a zero-voltage switching (ZVS) strategy to prevent voltage transients that may occur during switch turn-off due to leakage flux components of the inductors. The control and regulation of the light output of the LED lamps are achieved by applying double Pulse Width Modulation (PWM) signals to the switches. The proposed topology features relatively low power losses and improved voltage regulation. The simulation analysis and the projected driver-circuit results obtained in PSIM 9.0 are validated against prototype model results.

1. INTRODUCTION

Global energy consumption from lighting accounts for nearly one-fourth of total global energy consumption [1]. Due to their inherent merits, semiconductor-based components are used in various categories of lighting. It is more important to conserve energy than to produce it. The small-sized LED lamps demand low power and are durable. Hence, LED technology can be used to illuminate homes, industrial facilities, and commercial buildings [2,3]. The AC source-fed driver configuration for an LED light is of two categories: the two-stage driver and the single-stage driver [4]. The two-stage LED driver configuration first converts the AC source signal into a DC signal, which is then fed to the LED after it is processed by a boost power factor correction converter and a DC-DC converter stage. The two-stage structure, however, requires more active and passive components and a complex control strategy [5].

Due to the above-mentioned drawbacks in the two-stage LED driver structure, the researchers aimed to develop the single-stage LED driver configuration in which both the power factor correction as well as the LED's input current regulation functions are performed by a single DC-DC conversion stage [6,7]. The features, such as lower cost and simple control strategy, make the single-stage LED driver suitable for LED lighting applications [8,9].

The traditional DC-DC buck topology has the drawback that it is not possible to attain a very high step-down voltage conversion ratio at a duty cycle less than 10% due to poor utilization of semiconductor-based circuit components. The drawbacks of the conventional buck configuration are eliminated in the coupled inductor-based buck topology, in which the output voltage level can be reduced to a low value with fine-tuning of the duty cycle [10]. However, the coupled inductor's leakage inductance causes high-voltage spikes to appear across the power switch during turn-off [11,12]. The reduced switching losses and hence the improved converter efficiency for the coupled inductor-based converter structures can be achieved by employing the concept of soft switching technologies and the recycling of energy through the coupled inductors using a capacitor. Some researchers proposed resonant concept-based voltage divider circuits to be used in DC-DC converter circuits to reduce the switching losses [13]. However, the resonant-based voltage-dividing rule causes circuit components to fail due to the large magnitude of start-up surge currents.

The researchers have developed certain coupled inductor-based DC-DC converter topologies with soft switching techniques [14-25]. The high-power applications require the series-connected, parallel-connected, and series-parallel connected LEDs. When LEDs are connected in series, voltage balancing is important. If any one of the LEDs is damaged due to high voltage appearing across it, then the entire series string will fail [26]. Whereas, if the LEDs are to be connected in parallel, the balancing of current in each parallel path is important. Suitable current balancing is achieved using linear / switched current regulators [27,28]. The high step-down LED driver structures with multiple outputs are discussed by some authors in the literature [29-33].

The LED driver topologies discussed in the above paragraphs lead to the development of a high-efficiency and multiple-output DC-DC converter topology with a high step-down voltage conversion ratio suitable for LED driving applications. The work proposed in this paper explores a soft-switched and coupled-inductor-based single-input DC-DC buck configuration with dual output voltage levels. The projected topology has the characteristics of a high step-down voltage conversion ratio, reduced losses, and hence improved power conversion efficiency. The illumination control of the parallel-connected LEDs is also discussed. The design of the proposed LED driver is explored along with the current regulation of the parallel-connected LED string. The suggested cost-effective single-input and dual-output LED driver topology is a suitable choice for driving two LEDs, in which the illumination level of each LED is controlled by one active switch.

The work suggested in this paper is divided into different sections. Section 2 explores the modes of operation of the proposed LED driver structure along with the steady-state behavior of the topology. The double PWM control scheme is also briefed in Section 2. Section 3 illustrates the PSIM simulation model of the LED driver and the results. The prototype LED driver model and the corresponding results are presented in Section 4. Section 5 concludes the features of the suggested research work.

2. THE PROPOSED LED DRIVER TOPOLOGY

There are two DC-DC converters, namely the traditional

[1] Government College of Engineering Srirangam, Tiruchirappalli, India. Email: muralid@gces.edu.in

DOI: 10.59277/RRST-EE.2026.1.11

step-down converter and the coupled-inductor based step-down converter portions having common DC input source (V_s), integrated to configure the proposed LED driver structure with dual outputs V_{L1} and V_{L2} respectively as shown in Fig.1. The topology consists of semiconductor based components such as two active switches (main switch S_m with duty factor k_m and auxiliary switch S_a with duty factor $k_a \approx 1\text{-}k_m$) and two diodes (D_1 and D_2), and the passive components such as a capacitor (C_e) for recycling of energy, a coupled-inductor with primary winding of N_p turns and secondary winding of N_s turns and of inductances L_p and L_s respectively, an auxiliary inductor of inductance L_a, and two output capacitors of capacitances C_1 and C_2 respectively. The coefficient of coupling K_{CL} of the coupled inductor is taken as 1 since it is assumed that all the flux produced by the primary winding also links the secondary winding. The cross-regulation issue of the coupled inductor is minimized by choosing a very low value of the leakage inductance of the primary and secondary windings of the coupled inductor. In the proposed work, the leakage inductance is considered negligible. The proper and suitable management of leakage flux will reduce the effect of cross-coupling. Moreover, the double PWM technique plays a significant role in minimizing the above issues.

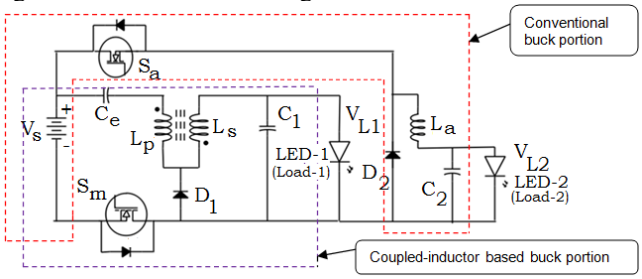

Fig. 1 – Power circuit of the projected LED driver topology.

The principle of operation of the projected single-input-dual-output LED driver topology is described by means of various operating modes as illustrated below.

The Mode-I operation commences with the turn ON condition of the main switch S_m and the turn OFF condition of the auxiliary switch S_a. As the anode of the diode D_1 is at a negative potential, it is reverse-biased, and hence it acts as an open circuit, as shown in Fig. 2. The leakage current of the coupled inductor rises as it gets charged from the supply voltage V_s through the capacitor C_e. The coupled inductor with two inductances, L_p and L_s, is now connected in series with the capacitor C_e. Most of the input voltage V_s gets dropped across the series-connected C_e, L_p, and L_s elements. The rest of the voltage V_s is now appearing across the capacitor C_1 to charge it, and hence the LED-1 is made to conduct. The previously charged auxiliary inductor L_a is now allowed to discharge its energy through the LED-2 and the capacitor C_2 by forward biasing the diode D_2. Thus, during mode-I, the LED-1 and LED-2 glow as they are in forward biased condition. When the main switch S_m is turned off at any instant, the Mode-I operation of the LED driver is complete. The voltage balance equation in Mode-I is written as:

$$V_s = V_{Ce} + V_{Lp} + V_{Ls} + V_{L1}, \quad (1)$$

$$V_{Lp} = V_{Ls}\left(\frac{N_p}{N_s}\right) = \frac{V_{Ls}}{n}, \quad (2)$$

$$V_s = V_{Ce} + V_{Ls}\left(\frac{n+1}{n}\right) + V_{L1}, \quad (3)$$

$$V_{Ls} = n\left(\frac{V_s - V_{Ce} - V_{L1}}{1+n}\right). \quad (4)$$

The flux balance equation for the secondary inductor L_s is written as:

$$n\left(\frac{V_s - V_{Ce} - V_{L1}}{1+n}\right) k_m T_s = V_{L1}\,(1-k_m)T_s, \quad (5)$$

where, $V_{Ce} = (V_{L1}/nk_m)$ and $n = N_s/N_p$.

Hence, the output voltage across LED-1 (V_{L1}) is derived as:

$$V_{L1} = \frac{nk_m}{(1-k_m)+(1+n)} V_s. \quad (6)$$

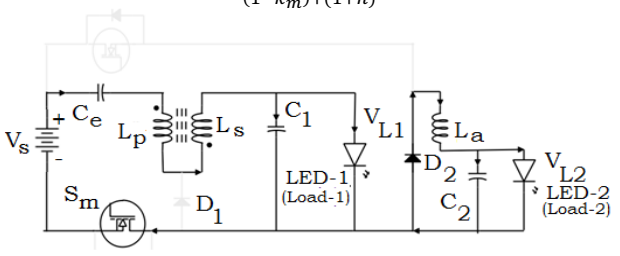

Fig. 2 – Mode-I operation of the proposed LED driver topology.

During Mode-II configuration, as depicted in Fig. 3, both the switches S_m and S_a are turned OFF. The junction capacitance C_m of the main switch is charged to the supply voltage V_s, and the junction capacitance C_a of the auxiliary switch discharges its energy until its voltage becomes zero. Both the capacitances C_m and C_a are assumed to be equal. The optimum choice of C_m and C_a can ensure Zero Voltage Switching (ZVS) operation of the switches S_m and S_a. The secondary inductor L_s starts discharging its energy by forward biasing the diode D_1, and hence the capacitor C_1 gets charged. Now the LED-1 is powered by the capacitor C_1. The auxiliary inductor L_a continues to discharge its energy through the capacitor C_2, by forward biasing the diode D_2. Now the capacitor C_2 gets charged and hence the LED-2 is powered.

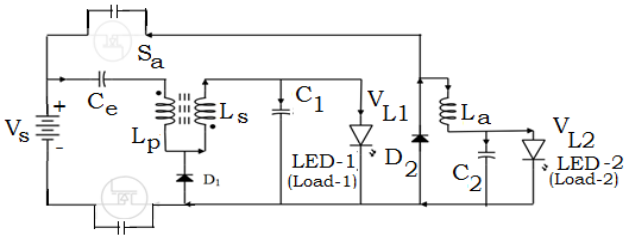

Fig. 3 – Mode-II operation of the proposed LED driver topology.

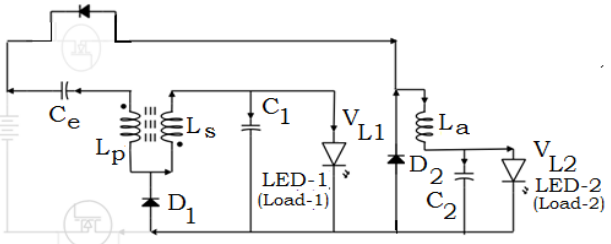

Fig. 4 – Mode-III operation of the proposed LED driver topology.

Figure 4 elucidates the Mode-III equivalent circuit in which the main switch S_m remains in a turned-off condition. The switch S_a has zero voltage applied across it, and the body diode of S_a is conducting to discharge the stored energy of the primary leakage inductor. The device D_2 remains in forward-biased condition so that the stored energy in the inductor L_a powers the LED-2. The forward biasing of the device D_1 makes the LED-1 glow due to the stored energy released from the secondary inductor L_s.

The conduction of the body diode of S_a in the previous mode makes it turn ON at zero voltage during Mode-IV operation, as

shown in Fig. 5. Hence, the ZVS operation of the switch S_a is ensured. The main switch S_m remains in the turned OFF condition. Devices D_1 and D_2 remain short-circuited by forward bias. Both the LED-1 and LED-2 glow due to the energy supplied by the inductors L_s and L_a, respectively, through the devices D_1 and D_2.

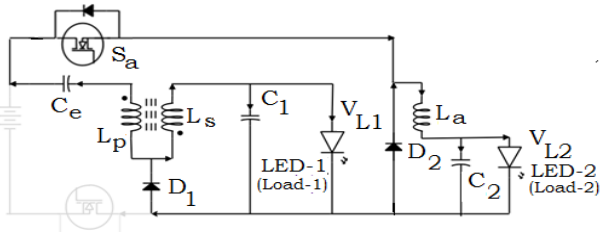

Fig. 5 – Mode-IV operation of the proposed LED driver topology.

During Mode-V operation, as illustrated in Fig. 6, device D_2 is open-circuited under reverse bias, and the inductor L_a is fully demagnetized. Now the inductor L_a is charged, through the conducting switch S_a, by the leakage inductor current on the primary side, and hence the LED-2 glows. Switch S_m remains in the OFF state. The LED-1 glows due to the discharge of the inductor L_s through the conducting diode D_1.

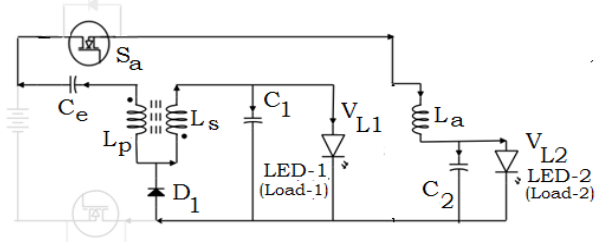

Fig. 6 – Mode-V operation of the proposed LED driver topology.

The switch S_a is turned OFF during Mode-VI operation. Now, the junction capacitance C_a is charged to the source voltage V_s, and the junction capacitance C_m gets completely discharged to zero voltage. At the subsequent Mode-VII, the capacitance C_a is open-circuited due to the fully charged condition, and the body diode of the switch S_m starts conducting, which ensures ZVS turn-on of the switch S_m during Mode-VIII. During Modes VI, VII, and VIII, LEDs 1 and 2 glow, receiving energy from inductors L_s and L_a, respectively.

In all the LED operating modes explained in above paragraphs, the double PWM approach for ZVS operation of the power switches enables independent regulation of the light-output brightness (luminous flux) and chromaticity of the two parallel-connected LEDs by decoupling effect of power conversion from dimming control, and by controlling the each LED branch current independently using separate PWM signals with suitable variation of duty cycle. This PWM scheme causes efficiency optimization across the whole operating range, prevention of color shifts, and component stress reduction [34–36].

For deducing the expressions for the voltage gains of the suggested LED driver topology, the operation of the topology under Mode I, Mode IV, and Mode V is considered. The flux balance concept is applied to the secondary inductor L_s and the auxiliary inductor L_a. The flux balance equation for the secondary inductor L_s is already written as eq. (5) for the switching period T_s. Similarly, the flux balance equation for the auxiliary inductor L_a is written as eq. (7) below for the same switching period T_s. Then the eq. (5) and (7) are used to derive the voltage gains (G_{L1} and G_{L2}) due to LED-1 and LED-2.

$$(-V_{L2})k_aT_s + (V_{Lp} + V_{Ce} - V_{L2})(1-k_a)T_s = 0, \quad (7)$$

$$G_{L1} = G_{LED\text{-}1} = \frac{V_{L1}}{V_s} = \frac{nk_m}{(1\text{-}k_m)+(1+n)}V_s, \quad (8)$$

$$G_{L2} = G_{LED-2} = \frac{V_{L2}}{V_s} = \frac{(1-k_a)}{6}. \quad (9)$$

3. PSIM SIMULATION MODEL OF THE SUGGESTED LED DRIVER AND THE RESULTS

The PSIM (POWERSIM 9.0) software tool is employed for the simulation of the projected LED driver topology. The corresponding simulation model of the LED driver operating at 100 kHz switching frequency is shown in Fig. 7. The loads are indicated as LED-1 and LED-2. The design specifications of the inductive and capacitive elements, and the input voltage (V_s) used for simulation are as shown in Table 1. The switching pulse for the main switch S_m is generated using double PWM strategy at 60% dimming of LED, by comparing the high frequency pulse (V_{gH}) at 100 kHz frequency and the low frequency pulse (V_{gL}) at 1 kHz frequency as shown in Fig. 8. The PWM signals as shown in Fig. 11 for the auxiliary switch S_a are generated at 90% dimming of LED either by complement operation on the switching pattern of the main switch S_m or by utilizing a logic circuit as depicted in Fig. 7. The waveforms of output voltages and currents for LED-1 and LED-2 are illustrated in Fig. 9 and Fig. 10 respectively for 60% and 90% dimming control. The soft switching (ZVS) waveforms of the main and auxiliary switches are depicted in Fig. 12.

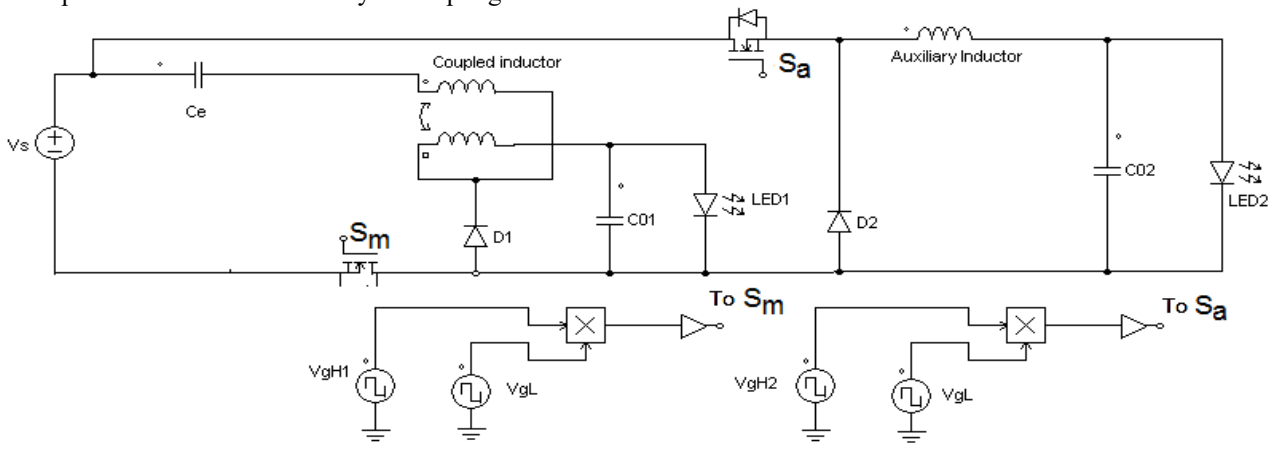

Fig. 7 – PSIM model of the suggested LED driver topology.

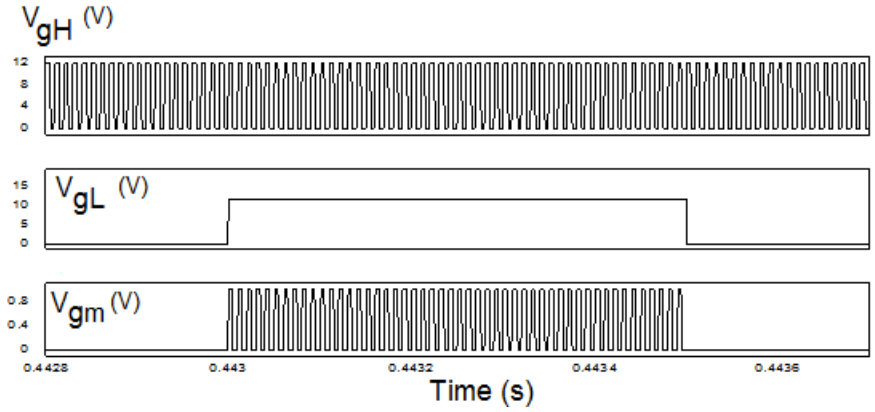

Fig. 8 – Switching pulse generation for the main switch S_m using the double PWM technique at 60% dimming.

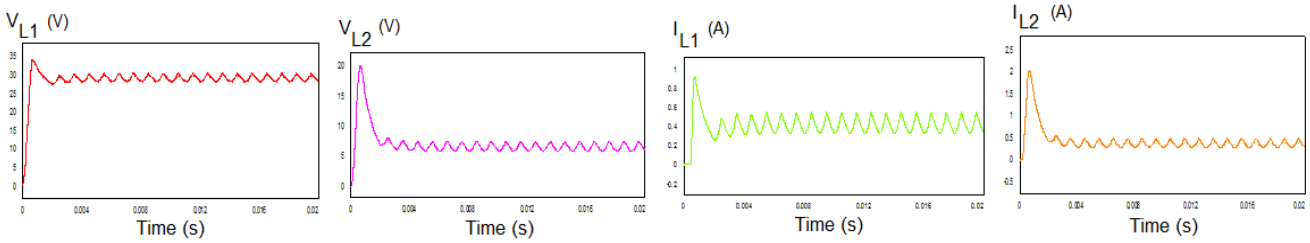

Fig. 9 – Output voltages (V_{L1} and V_{L2}) and output currents (I_{L1} and I_{L2}) for 60% dimming control.

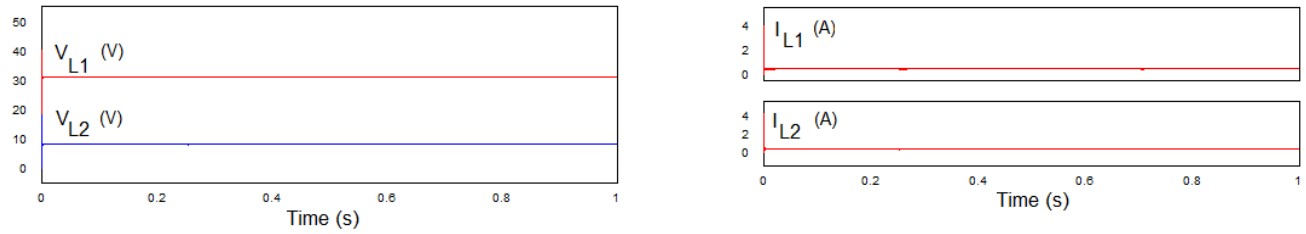

Fig. 10 – Output voltages (V_{L1} and V_{L2}) and output currents (I_{L1} and I_{L2}) for 90% dimming control.

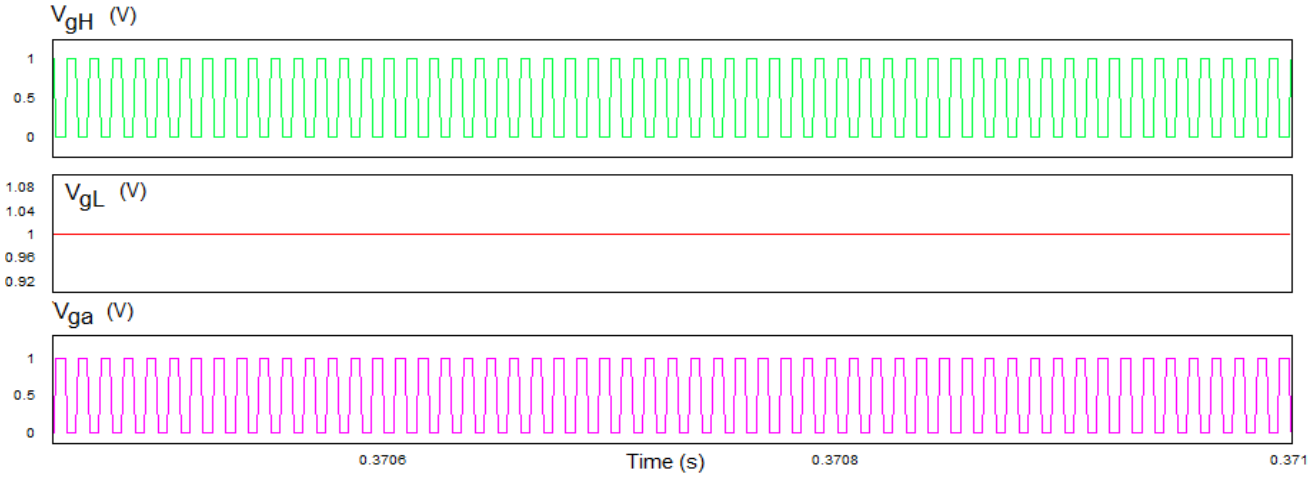

Fig. 11 – Switching pulses generation for the auxiliary switch S_a using the double PWM technique at 90% dimming.

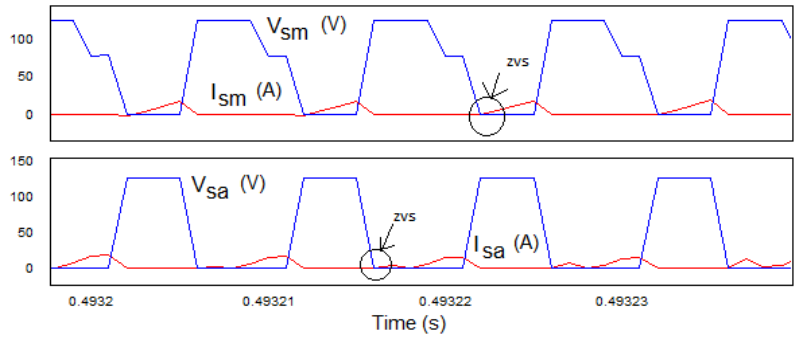

Fig. 12 – Soft switching (ZVS) waveforms for the main switch (S_m) and auxiliary switch (S_a)

Table 1

PSIM simulation model parameters and their values

Circuit parameters	Symbol	Value
DC input voltage to the LED driver	V_s	120 V
Primary inductor	L_p	1 mH
Secondary inductor	L_s	445 µH
Auxiliary Inductor	L_a	1.5 mH
Capacitor	C_e	1 µF
Capacitor	C_{01}	800 µF
Capacitor	C_{02}	60 µF
Switching frequency	f_s	100 kHz
Duty cycle (k) of the main and	k_m	0.6
auxiliary switches S_m & S_a	k_a	0.4
Output power	P_0	16 W

4. HARDWARE IMPLEMENTATION OF THE PROPOSED LED DRIVER AND THE RESULTS

The prototype model of the suggested LED driver of 10 W rating is developed as shown in Fig. 13 with a voltage capability of 5 V and a current capacity of 1 A. The prototype structure employs a magnetically coupled inductor with a tapping arrangement without the need for coupled and auxiliary inductors, so that the overall circuit is compact and highly efficient. The switching pulses are generated by means of an Arduino UNO microcontroller board based on ATmega328P. The Arduino IDE 1.8.1 is employed to develop the code for the double pulse width modulation (DPWM) technique. The AC power supply of 230 V, 50 Hz is stepped down to a low-level AC voltage of 15-0-15 V at 3 A using a step-down transformer with a centre-tap. Then, this low-voltage AC is rectified using 1N4007 diodes and filtered using a capacitor of 1000 µF/25V. The main and auxiliary switches S_m and S_a are of IRF 540 category of MOSFET, and each switch is driven by a transistor-based push-pull configuration. The UF5408 ultrafast feedback diodes and 2200 µF/50V rated capacitors are used at the output stage of the coupled inductor. The two LEDs, each rated 5 V / 1 A, act as loads. The switching pulses generated by the DPWM method for the main and auxiliary switches S_m and S_a are shown as V_{gH} (High frequency pulse) and V_{gL} (low frequency pulse) in Fig. 14 and Fig. 15, respectively. The waveform of voltage appearing across the two LEDs is depicted in Fig. 16.

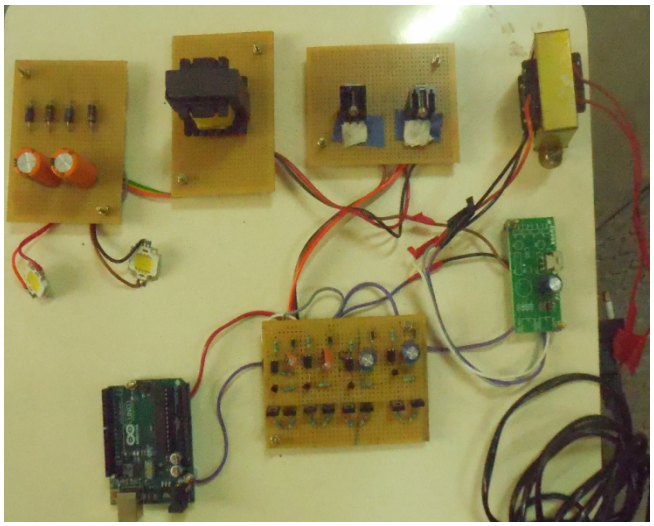

Fig. 13 – Prototype model of the projected LED driver topology

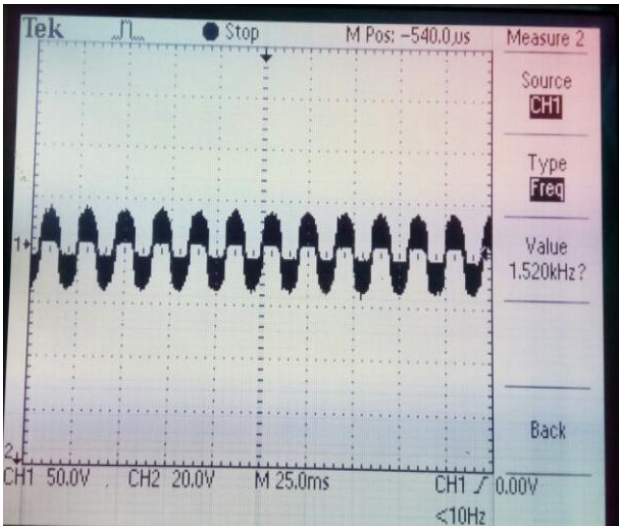

Fig. 14 – Gating pulses for the switches using the double PWM method – V_{gH} high pulse

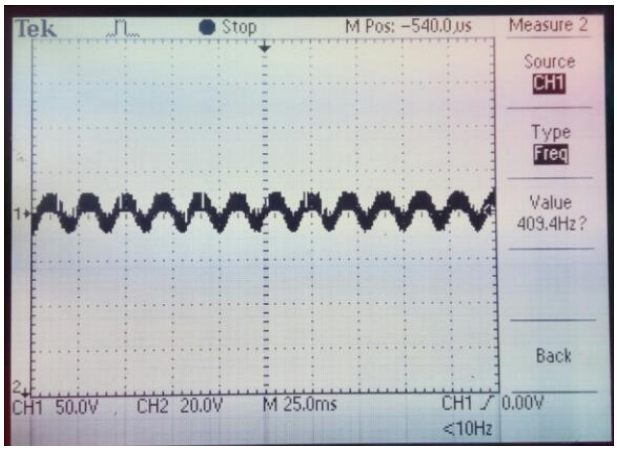

Fig. 15 – Gating pulses for the switches using the double PWM method – V_{gL} low pulse

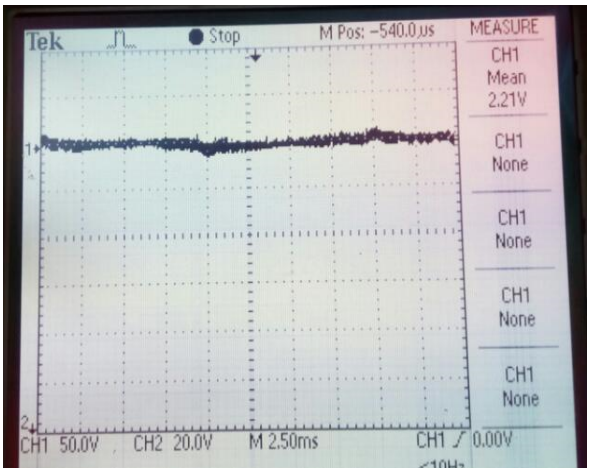

Fig. 16 – Load voltage ($V_{L1,}$ or V_{L2}) across two LEDs

5. CONCLUSIONS

The research concept proposed in this article explores the operational behavior during different modes of an efficient buck converter-driven LED lighting configuration with color stability. The projected LED driver structure employs one main power switch and one auxiliary power switch, one coupled inductor, a smaller number of passive components, and diodes. The power switches are controlled by ZVS to reduce switching losses. The PSIM simulation model of the

topology and the results are presented. With one number of power switch, it is possible to increase the LED output stages by simply adding auxiliary inductor elements. Hence, the overall circuit size and the cost are reduced. The LED dimming control capability at various levels, for reduced power consumption, achieved by means of a double PWM scheme, is another significant feature of the topology. The double PWM strategy regulates the LED current and helps to achieve power factor correction at the input side. The experimental investigation of the proposed LED driver is also conducted by developing a prototype.

ACKNOWLEDGMENT

The author acknowledges the technical support provided by the Department of Electrical and Electronics Engineering, Government College of Engineering Srirangam, Tiruchirappalli, in carrying out the simulation and experimental works on the proposed LED driver topology.

Received on 26 December 2025

REFERENCES

1. D. Steigerwald, J.C. Bhat, D.C. Collins, R.M. Fletcher, M.O. Holcomb, M.J. Ludowise, P.S. Martin, S.L. Rudaz, *Illumination with solid state technology*, IEEE Journal of Selected Topics in Quantum Electronics, **8**, *2*, pp. 310–320 (2002).
2. B. Mrabet, A. Chammam, *Study and implementation of LED drivers with dimming capability*, Advances in Science, Technology and Engineering Systems Journal, **6**, *6*, pp. 130–136 (2021).
3. A.S. Kamat, R. Khosla, V. Narayanamurti, *Illuminating homes with LEDs in India: rapid market creation towards low-carbon technology transition in a developing country*, Energy Research and Social Science, **66**, pp. 1–13 (2020).
4. M. Esteki, S.A. Khajehoddin, A. Safaee, Y. Li, *LED systems applications and LED driver topologies: a review*, IEEE Access, **11**, pp. 38324–38358 (2023).
5. R. Gunabalan, *Overview of passive light-emitting diode driver circuits for street lighting*, Bulletin of Electrical Engineering and Informatics, **5**, *3*, pp. 307–314 (2016).
6. Y. Wang, W. Wang, D. Xu, *A single-stage LED driver for the street lighting system*, Przegląd Elektrotechniczny, **88**, *1*, pp. 250–254 (2012).
7. Y.H. Yan, H.L. Cheng, C.A. Cheng, Y.N. Cheng, Z.X. Wu, *A novel single-switch single-stage LED driver with power factor correction and current balancing capability*, Electronics, **10**, *11*, pp. 1–16 (2021).
8. C.A. Cheng, C.H. Chang, T.Y. Chung, F.L. Yang, *Design and implementation of a single-stage driver for supplying an LED street-lighting module with power factor corrections*, IEEE Transactions on Power Electronics, **30**, *2*, pp. 956–966 (2015).
9. M. Sridhar, R. Seyezhai, *Lifetime prediction of single-stage LED driver circuit using Bayesian belief network*, Revue Roumaine des Sciences Techniques, **68**, *4*, pp. 351–356 (2023).
10. Y.T. Yau, W.Z. Jiang, K.I. Hwu, *Step-down converter with wide voltage conversion ratio*, IET Power Electronics, **8**, *11*, pp. 2136–2144 (2015).
11. E. Babaei, Z. Saadatizadeh, *High voltage gain DC-DC converters based on coupled inductors*, IET Power Electronics, **11**, *3*, pp. 1–19 (2018).
12. A.K. Paul, B. Sai Ram, S.V. Kulkarni, *Review of coupled inductors in power electronics: from concept to practice*, e-Prime – Advances in Electrical Engineering, Electronics and Energy, **8**, pp. 1–14 (2024).
13. K.I. Hwu, Y.T. Yau, *A buck resonant voltage divider with bidirectional operation considered*, IEEE Transactions on Industry Applications, **49**, *4*, pp. 571–578 (2011).
14. M. Maalandish, E. Babaei, P. Abolhasani, M. Gheisarnejad, M.H. Khooban, *Ultra high step-up soft-switching DC/DC converter using coupled inductor and interleaved technique*, IET Power Electronics, **16**, *8*, pp. 1320–1338 (2023).
15. S.R. Addula, P. Mahalingam, *Coupled inductor based soft switched DC-DC converter for PV applications*, International Journal of Renewable Energy Research, **6**, *2*, pp. 361–374 (2016).
16. N. Bagheri, H. Alipour, L. Mohammadian, J. Beiza, M. Ebadpour, *A new high step-down soft-switched DC-DC converter based on coupled inductor*, International Journal of Electronics, pp. 1–21 (2024).
17. G. Chen, L. Chen, Y. Deng, X. He, Y. Wang, J. Zhang, *Single coupled-inductor dual output soft-switching DC-DC converters with improved cross-regulation and reduced components*, IET Power Electronics, **10**, *13*, pp. 1665–1678 (2017).
18. E.H. Ismail, *Large step-down DC-DC converters with reduced current stress*, Energy Conversion and Management, **50**, *2*, pp. 232–239 (2009).
19. D. Lokesh, C. Senthilsingh, *Aquila optimized nonlinear control for DC-DC boost converter with constant power load*, Revue Roumaine des Sciences Techniques, **69**, *4*, pp. 419–424 (2024).
20. A. Farooq, M.Z. Malik, Z. Sun, G. Chen, *A review of non-isolated step-down DC-DC converters*, International Journal of Smart Home, **9**, *8*, pp. 133–150 (2015).
21. S. Khalili, H. Farzanehfard, M. Esteki, *High step-down DC-DC converter with low voltage stress and wide soft-switching range*, IET Power Electronics, **13**, *14*, pp. 3001–3008 (2020).
22. E. Alhani, F. Anayi, *The design of a hybrid DC/DC converter for LED lighting system using a single switch*, Energy Reports, **10**, pp. 4491–4502 (2023).
23. M.D. Vecchia, G.V. den Broeck, S. Ravyts, J. Driesen, *Novel step-down DC-DC converters based on the inductor-diode and inductor-capacitor-diode structures in a two-stage buck converter*, Energies, **12**, *6*, pp. 1–22 (2019).
24. D. Murali, *Analysis and experimental validation of a non-isolated DC-DC SEPIC-modified CUK combined converter*, Revue Roumaine des Sciences Techniques, **70**, *3*, pp. 367–372 (2025).
25. B. Lakshmi Praba, R. Seyezhai, *Flicker-free resonant DC-DC SEPIC converter with Valley-fill for LED applications*, Revue Roumaine des Sciences Techniques, **70**, *1*, pp. 47–52 (2025).
26. S.C. Hsia, J.J. Ciou, *Single chip design for detection and recovery of series LED open/short fault tolerance circuit*, IET Power Electronics, **11**, *15*, pp. 2434–2439 (2018).
27. R. Zhang, H.S.H. Chung, *Paralleled LED strings: an overview of current-balancing techniques*, IEEE Industrial Electronics Magazine, **9**, *2*, pp. 17–23 (2015).
28. H.L. Cheng, Y.C. Hung, *A high power factor LED driver with intrinsic current balancing capability*, Applied Sciences, **13**, *12*, pp. 1–16 (2023).
29. Q. Luo, B. Zhu, W. Lu, L. Luowei, *High step-down multiple-output LED driver with the current auto-balance characteristic*, Journal of Power Electronics, **12**, *4*, pp. 519–527 (2012).
30. M. Ganga, G. Jasmine, N. Muthukumaran, M. Veluchamy, *Red Fox-based fractional order fuzzy PID controller for smart LED driver circuit*, Revue Roumaine des Sciences Techniques, **68**, *4*, pp. 394–399 (2023).
31. B. Zhu, Q. Luo, Y. Wang, L. Zhou, *High step-down constant current LED driver with multiple outputs*, Diangong Jishu Xuebao/Transactions of China Electrotechnical Society, **28**, *6*, pp. 178–183 (2013).
32. M. Esteki, S.A. Khajehoddin, A. Safaee, Y. Li, *LED systems applications and LED driver topologies: a review*, IEEE Access, **11**, pp. 38324–38358 (2023).
33. V. Teodor-Iulian, S. George-Călin, E. Bogdan-Adrian, *Analysis and bidirectional DC-DC power converters for screening systems of retired batteries*, Revue Roumaine des Sciences Techniques, **69**, *3*, pp. 311–316 (2024).
34. H.J. Chiu, Y.K. Lo, Y.L. Lin, G.C. Jane, *A cost-effective dimming method for LED lighting applications*, International Journal of Circuit Theory and Applications, **43**, *3*, pp. 307–317 (2015).
35. C.S. Moo, Y.J. Chen, W.C. Yang, *An efficient driver for dimmable LED lighting*, IEEE Transactions on Power Electronics, **27**, *11*, pp. 4613–4618 (2012).
36. M.W. Umar, N.B. Yahaya, Z.B. Baharuddin, *PWM dimming control for high brightness LED-based automotive lighting applications*, International Journal of Electrical and Computer Engineering, **7**, *5*, pp. 2434–2440 (2017).